

## Nonlinear dynamical modeling of adsorption and desorption processes with power-law kinetics: Application to CO<sub>2</sub> capture

Vincent Tartaglione, Christophe Farges<sup>✉,\*</sup> and Jocelyn Sabatier<sup>†</sup>

*IMS Laboratory, Bordeaux University, UMR CNRS 5218–351, Cours de la Libération, 33405 Talence Cedex, France*



(Received 18 June 2020; accepted 10 October 2020; published 2 November 2020)

Modeling of random sequential adsorption (RSA) process is studied in this paper as this kind of process is close to the surface adsorption phenomenon that is, for instance, exploited in gas sensors or for liquid or gas purification. Analysis and simulation of the RSA process is first performed to highlight a power-law kinetic behavior. Such behaviors are often modeled in the literature with fractional models. The paper, however, shows that fractional models are not able to capture some important properties of the RSA process. A nonlinear model and the associated parameters tuning method are, thus, proposed. A discussion on the ability of the proposed model to capture the power-law kinetics without exhibiting some of the drawbacks of fractional models is proposed. This nonlinear model is then modified to take into account the reverse desorption process. The proposed modeling approach is applied to experimental data of CO<sub>2</sub> capture.

DOI: [10.1103/PhysRevE.102.052102](https://doi.org/10.1103/PhysRevE.102.052102)

### I. INTRODUCTION

In chemistry, adsorption is a surface phenomenon in which atoms, ions, or molecules (adsorbates) attach to a solid surface (adsorbent) from a gaseous, liquid, or solid solution. This process is based on the interaction of the adsorbate with a surface, which can involve various, more or less intense, processes, such as Van der Waals interactions [1], dipolar interactions, covalent, or ionic chemical bonds [2].

This phenomenon is widely used in academic applications in physical, chemical, or biological domains to capture pollutants, gas separation, catalysts, and so as a rule remove a substance from a liquid or gaseous solutions [3]. Adsorption phenomenon is also widely used in industry especially for water purification [3] but also in many other applications (e.g., [4,5]), such as sensor design [6,7]. It is, therefore, essential to characterize this phenomenon and its associated kinetics and to have efficient tools to model these kinetics.

In this paper, the authors consider first an idealized adsorption process called random sequential adsorption (RSA) in two dimensions (2D), which is close to the surface chemical adsorption phenomenon previously cited. The RSA process has been studied since the early 20th century first in one dimension independently by Flory [8] and Rényi with the denoted car-parking problem [9]. The 2D process was studied in Refs. [10–12] in which the kinetic behavior and the particle concentration final value were investigated.

Then this paper focuses on the kinetics of the adsorption process. Several models were proposed in the literature for these kinetics. An interesting analysis of these models is proposed in Ref. [13]. If  $q(t)$  denotes the amount of adsorbed particles, most of the discussed models express the adsorption rate  $\frac{dq(t)}{dt}$  as a function of the distance  $q_e - q(t)$ , where  $q_e$

denotes the amount of adsorbed particles at the equilibrium.

The following models have been proposed:

(1) by Lagergren [14],

$$\frac{dq(t)}{dt} = k_1[q_e - q(t)],$$

(2) by Kopelman [15],

$$\frac{dq(t)}{dt} = k_2 t^{-h}[q_e - q(t)] \quad \text{with } 0 \leq h \leq 1,$$

(3) by Ho and McKay [16],

$$\frac{dq(t)}{dt} = k_3[q_e - q(t)]^2,$$

(4) by Brouers and Sotolongo-Costain [17],

$$\frac{d^\alpha q(t)}{dt^\alpha} = k_4[q_e - q(t)]^n.$$

If  $\theta(t) = \frac{q(t)}{q_m}$  denotes the relative surface coverage, where  $q_m$  is the maximal amount of adsorbed particles and if  $c$  denotes the concentration of particles close to the surface (bulk), the following model was also proposed by Haerifar and Azizian [18] and Bashiri and Shajari [13],

$$\frac{d\theta(t)}{dt} = k_5 t^{-h} c [1 - \theta(t)] \quad \text{with } 0 \leq h \leq 1.$$

The most realistic model seems to be the last one as the previous ones do not take into account explicitly the particle concentration near the surface. On the other hand, if we consider an analogy between the physical adsorption and the idealized RSA process (see Sec. II), a thorough study [10,12,19] of the RSA process reveals that the “fractal-like” behavior introduced in Refs. [13,18] under the form of the  $t^{-h}$  factor does not hold during all the process but is valid only asymptotically when packing is close to saturation limit. Thus, it should not be used to fit kinetics at the beginning of the packing formation. Moreover, their model has a singularity at time  $t = 0$ .

\* christophe.farges@u-bordeaux.fr

† jocelyn.sabatier@u-bordeaux.fr

In the following to some results presented in Ref. [20], the main goal of this paper is to propose a new model for adsorption kinetics in a physical time in accordance with the kinetic behavior observed in the RSA process and without the limitations of the models previously cited, and to apply this new model on real data. To this purpose, several known properties of the 2D RSA process are first recalled. As this process kinetic exhibits a power-law behavior, a fractional order model is naturally first studied. For a constant flow of particles, it permits a nice fitting of the 2D RSA kinetics but is not compatible with the process for a null flow and is of infinite dimension (thus, requiring an infinite number of initial conditions). To address this problem, a drift less input affine nonlinear model (or distributional model) is proposed. This kind of model was previously proposed in the literature to take into account the different types of kinetics that appear for low and high surface coverages. A theoretical justification of this class of model appears in Ref. [21]. The proposed model for RSA kinetics of anisotropic particles is based on the available surface function concept and is defined by

$$\frac{d\theta(t)}{dt} = \frac{1}{2\pi} \int \Phi[\theta(t), \Omega] d\Omega, \quad (1)$$

where  $\Phi[\theta(t), \Omega]$  is the probability of adding a new particle with orientation  $\Omega$  to the surface when the coverage is  $\theta(t)$ . The function  $\Phi[\theta(t), \Omega]$  cannot be obtained exactly, but approximations can be computed under the form of series expansions for low and high coverage regimes. These two approximations are then combined to provide an approximate description of the kinetics over the entire coverage range. The following two interpolation formulas are proposed in Ref. [21],

$$\Phi(\zeta) = (1 - \zeta)^4 (1 + c_1 \zeta + c_2 \zeta^2) \quad \text{with} \quad \zeta = \frac{\theta(t)}{\theta_\infty}, \quad (2)$$

and

$$\Phi(\zeta) = \frac{(1 - \zeta)^4}{(1 + c_1 \zeta + c_2 \zeta^2)}. \quad (3)$$

Parameters  $c_1$ ,  $c_2$ ,  $d_1$ , and  $d_2$  are then computed to fit the series expansions of the function  $\Phi[\theta(t), \Omega]$  in (1). An expansion similar to (2) is used in Refs. [22,23],

$$\Phi(\zeta) = (1 - \zeta)^4 (1 + c_1 \zeta + c_2 \zeta^2 + c_3 \zeta^3). \quad (4)$$

In Ref. [22], parameters  $c_1$ ,  $c_2$ , and  $c_3$  are computed as in Ref. [21] and to fit insulin adsorption data as Ref. [23]. These works, and particularly Ref. [21], fully justify the interest of nonlinear models for RSA kinetic modeling and by extension for adsorption kinetics in physical time. However, these models have a constrained form to meet the asymptotic behaviors for low and high surface coverage which reduces the accuracy of the model outside these coverage regimes.

In our approach a more general expansion is considered in model (1). The tuning method associated with this model is detailed, and its efficiency is proved. In order to get closer to the possible physical application, a rate of desorption not considered in Refs. [21–23] is also finally added to the model. In the last section, it is shown that the model and the method described in this article can be applied to real data. Data of

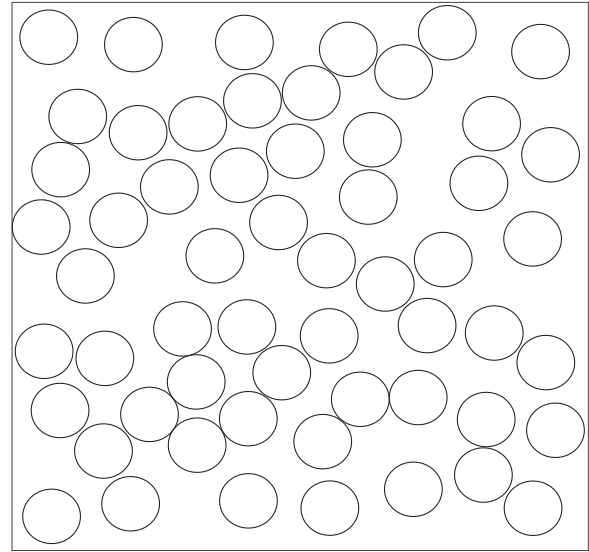


FIG. 1. A partially filled surface.

adsorption and desorption of CO<sub>2</sub> on copper hexacyanoferrate controlled by N<sub>2</sub> are, thus, analyzed and modeled.

## II. RANDOM SEQUENTIAL ADSORPTION

### A. Presentation of the process

In this section is described the random sequential adsorption process (denoted in the following RSA process) studied in the paper. Random sequential adsorption was widely studied in the literature ([24–26]). In this paper, the substrate in which particles adsorb is a square on the plane with edge length  $L$  and with corresponding area  $L^2$ . Adsorption of discs particles of radius  $R$  ( $R \ll L$ ) on the surface is considered. The particles sequentially incide at uniformly randomly chosen surface positions. The particles are supposed moving in the perpendicular direction of the plane at each iteration of the process. A particle attaches to the surface only if the target sites is empty, i.e., if all the surface occupied by the incident particle correspond to an empty site at the substrate. Otherwise, the adsorption attempt is rejected, and the disk goes back. At the initial time  $t_0$ , the adsorption surface is empty. In the following  $t_k$  denotes the iteration number (also called time) at which the  $k$ th particle tries to attach to the surface and let  $\Delta t = t_{k+1} - t_k$ .

In Fig. 1, an example of the process is illustrated. The surface is yet not completely filled with disks. Figure 2(left) shows a region in which adsorption is impossible, and Fig. 2(right) shows a region in which adsorption is possible.

The density of occupied area is noted  $\theta(t)$ . The value of  $\theta(t)$  when  $t$  goes to infinity is denoted  $\theta_\infty$ . According to the literature ([12,27,28]), numerical simulations lead to the following value for  $\theta_\infty$ :

$$\theta_\infty = \lim_{t \rightarrow \infty} \theta(t) \approx 0.547. \quad (5)$$

### B. Simulation of the process

In order to simulate this process, a (pseudo) random couple  $c = (p, q)$  of real numbers that follows a uniform distribution

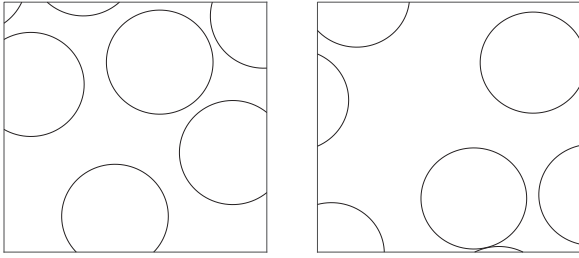


FIG. 2. Two cases of adsorption on the surface: Subregion of Fig. 1 where adsorption is impossible (left), and subregion of Fig. 1 where adsorption is possible (right).

in range  $[0, L]$  is generated at each iteration of the process. A disk of radius  $R$  and center  $c$  will fix on the surface if:

(1) A part of the disk does not lie outside the surface, which is true if the following two conditions are satisfied:  $p, q \geq R$  and  $p, q \leq L - R$ ;

(2) there is no overlap between the current disk and a previously fixed disk, that is if  $d(c, c_k) \geq 2R$  where for all  $k \in \mathbb{N}$ ,  $c_k = (p_k, q_k)$  is the center of a disk previously fixed on  $S$  and where  $d(c, c_k) = \sqrt{(p - p_k)^2 + (q - q_k)^2}$  is the distance between disks.

In Fig. 3 is plotted the density  $\theta$  of occupied area for  $R = 0.5$  and  $L = 50$  ( $\frac{L}{R} = 100$ ) as a function of trials which is denoted  $t$  in the following. If the flow of particles that hit the surface per second is constant,  $t$  is proportional to the real time. The final density value is here  $\theta_\infty \approx 0.5344$ . Since the goal of this paper is not to do a deep analysis of RSA, it is not relevant here to go any further, since the convergence is very slow, and the algorithm becomes really time consuming. About  $4 \cdot 10^6$  trials were needed to reach this value and the last different value before  $\theta_\infty = 0.5344$  was unchanged for 918 534 iterations. It was concluded that the jamming configuration was close enough to be reached. The error bars correspond to the fluctuations of the value at the given trial between several simulations of the process. These fluctuations are due to the randomness of the process.

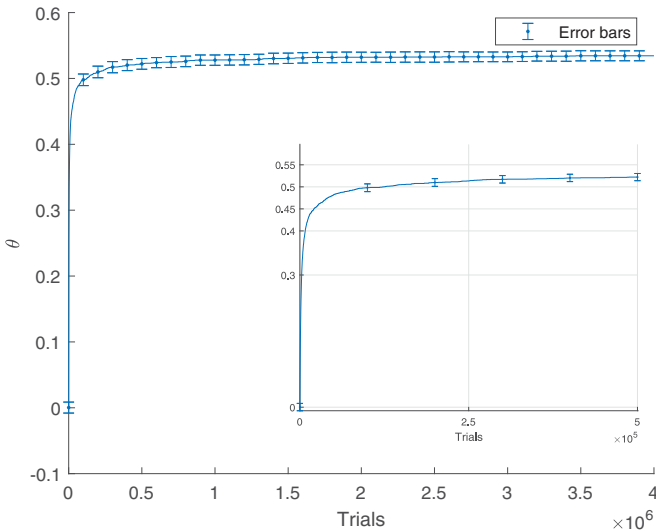


FIG. 3. Density of the occupied area as a function of trials.

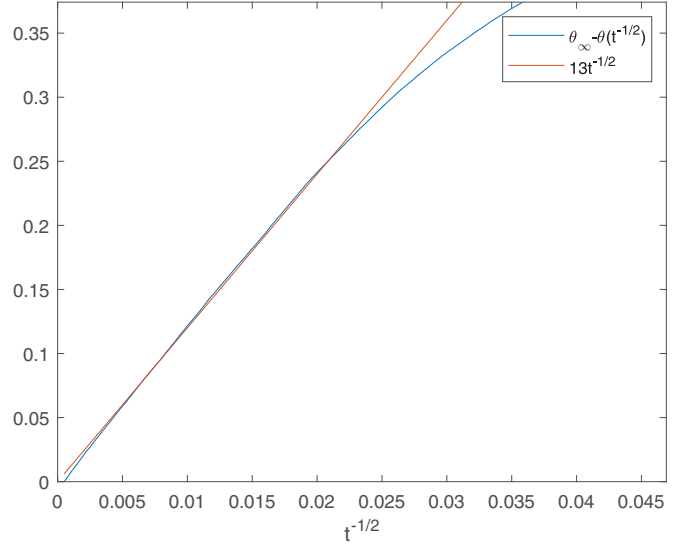


FIG. 4. Highlighting of the power law behavior of  $\theta_\infty - \theta$  for large values of  $t$ .

It is suggested in the literature [10,12,19] that the covered surface can be described for high coverage regimes by a power law,

$$\theta_\infty - \theta(t) \sim t^{-1/2}. \tag{6}$$

In order to confirm this statement,  $\theta$  is represented in Fig. 4 as a function of  $t^{-1/2}$ . For large enough values of  $t$  (small values of  $t^{-1/2}$ ), this figure highlights that  $\theta_\infty - \theta(t) \sim at^{-1/2}$  with  $a = 13$ . Note that this behavior only holds in a limited trials range. At the beginning due to the large number of free places  $\theta_\infty - \theta(t) \sim t$ .

*Remark 1.* Other simulations were performed for other  $\frac{L}{R}$  ratios in the range of  $50 < \frac{L}{R} < 1000$ . The high coverage kinetics (dynamics in  $t^{-1/2}$  for large values of  $t$ ) and final coverage density were the same in all cases, showing that the ratio considered above ( $\frac{L}{R} = 100$ ) is large enough.

### III. DYNAMICAL MODELING OF RSA

#### A. Fractional order modeling

Since a behavior in  $t^{-1/2}$  has been highlighted in Sec. II B, modeling using a fractional order model seems natural [29]. As shown in Fig. 5, the signal  $y(t) = \theta_\infty - \theta(t)$  is, thus, considered as the response of a dynamical system to a Heaviside step function [ $u(t) = 0 \forall t < 0$ ;  $u(t) = 1 \forall t \geq 0$ ]. The input  $u(t)$  of the system can, thus, be viewed as a particles flow of one particle per unit of time (trials). Based on the asymptotical behavior of the system, the following transfer function is used as the considered fractional model,

$$H(s) = \frac{sK}{\left(\frac{s^\alpha}{\omega_b} + 1\right)\left(\frac{s^{1-\alpha}}{\omega_h} + 1\right)}. \tag{7}$$

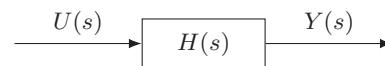


FIG. 5. Input-output representation of the system.

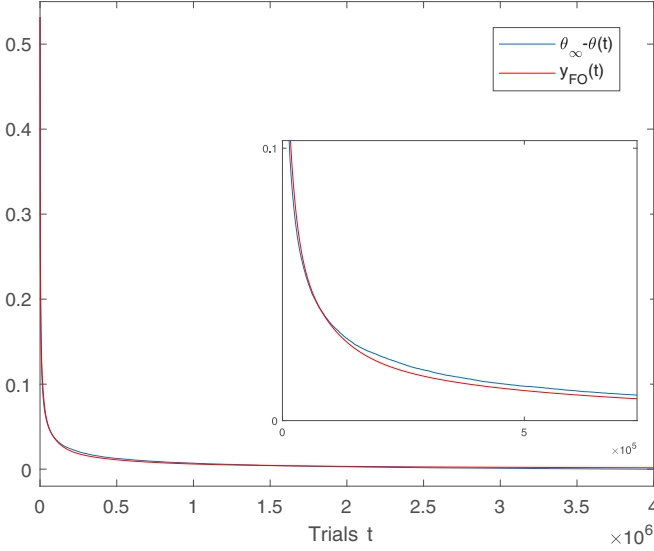


FIG. 6. Density of free area (in blue) and response of the fractional model (in red).

The constant  $K$  is related to the initial value of  $y(t)$ . Indeed, according to the initial value theorem,

$$y_0 = \lim_{t \rightarrow 0} y(t) = \lim_{s \rightarrow \infty} sY(s) = \lim_{s \rightarrow \infty} sH(s) \frac{1}{s} = \frac{K}{\omega_b \omega_h}. \quad (8)$$

Hence,

$$K = \frac{y_0}{\omega_b \omega_h}. \quad (9)$$

The fractional order  $\alpha$  and the constants  $\omega_b$  and  $\omega_h$  are obtained by minimizing the following criterion (least-squares optimization) that is nonlinear with respect to the parameters:

$$C = \frac{1}{N} \sum_{k=1}^N |y(k) - y_{FO}(k)|^2, \quad (10)$$

where  $y_{FO}$  denotes the model (7) step response. The following parameters were obtained:  $\alpha = 0.52$ ,  $\omega_b = 0.0145 \text{ rad s}^{-1}$ , and  $\omega_h \simeq 6.1542 \times 10^{-4} \text{ rad s}^{-1}$ . In Fig. 6 is proposed a comparison of model (7) step response  $y_{FO}$  with  $y$  obtained by the implementation of RSA process. The criterion (10) value is as follows:

$$C_1 = 2.7013 \times 10^{-6}. \quad (11)$$

### B. Discussion on fractional order modeling

At first look, this model seems effective in order to describe the kinetic of the density  $\theta(t)$ . However, there exist some limitations on the capacity of the model to capture some properties of the process described in Sec. II A.

Indeed, the RSA process is nonlinear. If the flow of particles is doubled, the filling dynamic of the surface is almost doubled, but the final value is the same as for a single flow as illustrated in Fig. 7. However, as the fractional order model is linear, if the flow is doubled, the final value will be doubled as well.

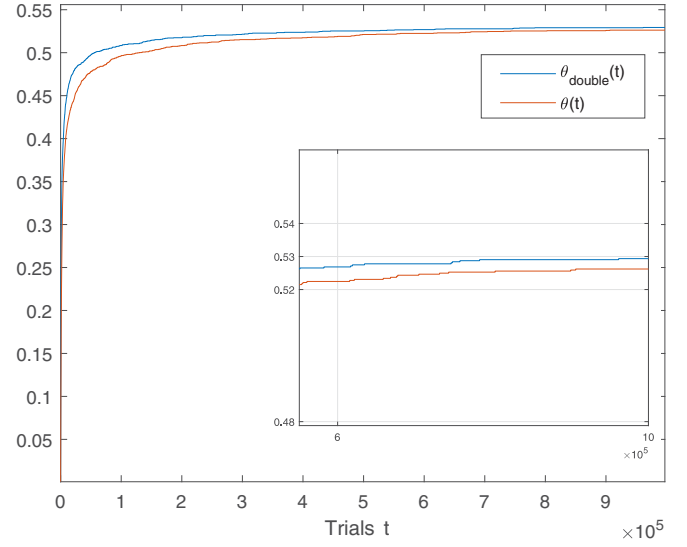


FIG. 7. Comparison between the dynamic  $\theta_{\text{double}}(t)$  of the process for a doubled flow of particles (blue) and a for a single flow of particles (orange).

Moreover, with the RSA process if the flow is stopped then the filling is obviously stopped. And if the flow restarts, the filling will restart at the same point. To reach such a behavior, model (3) must be transformed. Using this model, it is possible to write that

$$\theta(s) \left( \frac{s}{\omega_h \omega_b} + \frac{s^\alpha}{\omega_b} + \frac{s^{1-\alpha}}{\omega_h} + 1 \right) = U(s), \quad (12)$$

where  $U(s)$  is the flow of particles (linked to the concentration of particle near the surface). Relation (12) leads to the following differential equation:

$$\frac{d\theta(t)}{dt} = -\omega_h \frac{d^\alpha \theta(t)}{dt^\alpha} - \omega_b \frac{d^{1-\alpha} \theta(t)}{dt^{1-\alpha}} - \theta(t) + \omega_h \omega_b u(t). \quad (13)$$

The constancy of  $\theta(t)$  when the flow is zero can be obtained with a modification of relation (13) and by introducing a function  $v(t)$  such that,

$$\frac{d\theta(t)}{dt} = \left( -\omega_h \frac{d^\alpha \theta(t)}{dt^\alpha} - \omega_b \frac{d^{1-\alpha} \theta(t)}{dt^{1-\alpha}} - \theta(t) + \omega_h \omega_b u(t) \right) v(t), \quad (14)$$

with  $v(t) = 0$  if  $u(t) = 0$  and  $v(t) = 1$  if  $u(t) > 0$ .

However, such a modification does not solve the linearity problem with respect to the flow  $u(t)$  but above all, leads to using an infinite dimensional model which implies problems highlighted in Refs. [30–33] and to several other drawback discussed in Ref. [34] and summarized in Refs. [35,36]. It is, therefore, proposed to consider a nonlinear model to capture these properties.

### C. Nonlinear modeling

In order to capture the nonlinear behavior of the RSA process described in Sec. III B, the following model is considered:

$$\dot{y}(t) = f(y)u(t), \quad (15)$$

where

- (1)  $y: \mathbb{R}_+ \rightarrow \mathbb{R}_+$  is the density of free places on the surface as a function of time,  $y(t) = 1 - \theta(t)$ ;
- (2)  $u: \mathbb{R}_+ \rightarrow \mathbb{R}_+$  stands for the flow of particles;
- (3)  $f: \mathbb{R}_+ \rightarrow \mathbb{R}_+$  is a function to be determined.

This model is called a drift-free *control-affine system* or *affine-in-control system* [37,38]. It is clear that it has the property that if  $u(t)$  is doubled, the dynamic is also doubled. Note that the initialization of this model only requires the knowledge of  $y(0)$ . Physically the free place information is enough for the initialization of the process along with a stochastic distribution of the disk on the surface.

**1. Application on the simulated data**

Let  $k \in \mathbb{N}$ . For  $N \in \mathbb{N}$ ,  $k$  RSA processes of  $N$  trials are simulated. The output of the  $k$ th process is denoted  $Y_k$ . For all  $n \in \llbracket 0, N \rrbracket$ ,  $Y_k(n)$  is the density of free places on the surface according to the  $n$ th trial for the  $k$ th simulation. To approach the values of the unknown function  $y(t)$ , a large number of simulations is performed. The mean of these simulations is then considered.

More precisely, for all  $k \in \mathbb{N}$ ,  $Y_k$  is a random vector and for all

$i \in \mathbb{N}$ ,  $Y_k(i) \in [0, 1]$ . Then the sequence  $(Y_k)_{k \in \mathbb{N}}$  is bounded and the mean  $\mathbb{E}[Y_k]$  exists for all  $k \in \mathbb{N}$ . The sequence  $(Y_k)_{k \in \mathbb{N}}$  is a sequence of independent and identically distributed random vectors with mean  $\mathbb{E}[Y_0] = \mathbb{E}[Y_1] = \dots = \mu$ . By the strong law of large numbers, when  $k \rightarrow \infty$ ,

$$Y_{\text{mean}} = \frac{1}{k} \sum_{i=0}^k Y_i \rightarrow \mu = y(t), \quad \text{almost surely.} \quad (16)$$

With 200 simulations of the RSA process of  $4 \times 10^6$  trials, the curve of Fig. 8 is obtained. The number of 200 simulations has been chosen because with more than 200 simulations, changes in the mean value and behavior deviations is less than  $5 \times 10^{-5}$ . For all  $n \in \llbracket 0, N \rrbracket$ , the derivative  $\dot{y}$  of  $y$  is computed

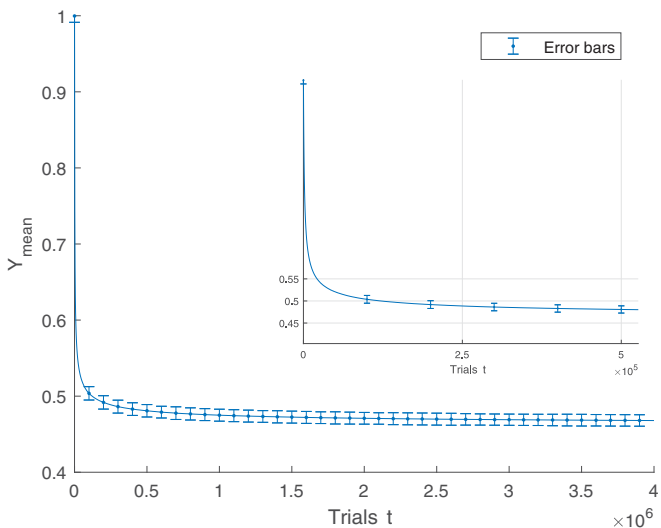


FIG. 8. Mean density of free area for  $u(t) = 1$ .

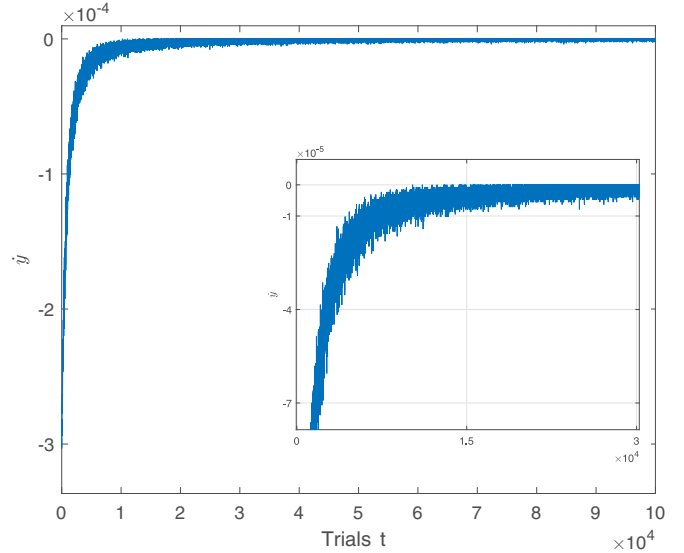


FIG. 9. Approximation of the derivative  $\dot{y}$ .

using the following formula and plotted in Fig. 9:

$$\dot{y}(n) \approx \frac{Y_{\text{mean}}(n+1) - Y_{\text{mean}}(n-1)}{2}. \quad (17)$$

The aim is now to find an analytical expression for function  $f$  in relation (15). In Fig. 10,  $\dot{y}$  is, thus, plotted as a function of  $y$  [considering that  $u(t) = 1$ ].

The curve of  $\dot{y}[y(t)]$  is then fitted using a least-squares method with the following function:

$$f(y) = a_0y + a_1y + a_2y^2 + a_3y^3 + a_4y^4. \quad (18)$$

The parameters  $a_0, a_1, a_2, a_3$ , and  $a_4$  given in Table I were obtained using MATLAB function FMINCON.

The comparison of  $f(y)$  with the approximation  $\dot{y}(y)$  computed previously is also represented in Fig. 10. The diagram in Fig. 11 is an implementation of relation (15) where function  $f$

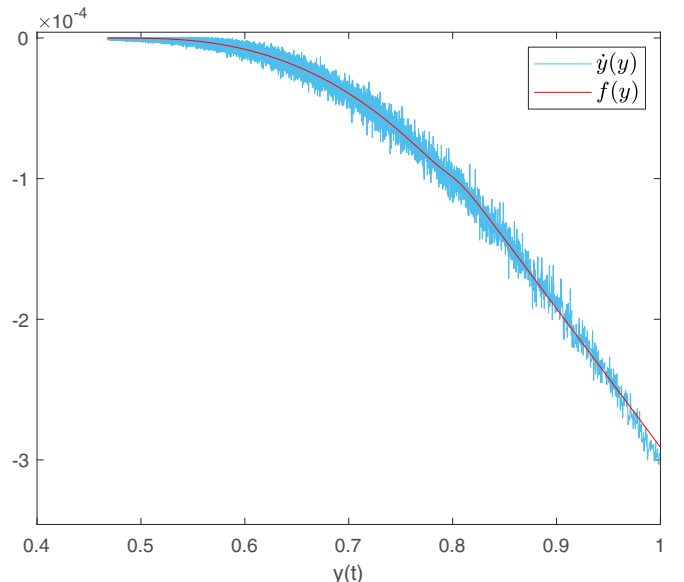


FIG. 10. Function  $\dot{y}[y(t)]$  and its approximation.

TABLE I. Parameters of  $f$  from relation (18).

$a_0$	$a_1$	$a_2$	$a_3$	$a_4$
$2.8163 \times 10^{-4}$	$-9.4715 \times 10^{-4}$	$-6.4938 \times 10^{-4}$	0.0050	-0.0043

is given by relation (18). Such a diagram is used for simulation of the density of free space as a function of time.

In Fig. 12 is proposed a comparison of model (15) response for  $u(t) = 1$ , denoted  $Y_{\text{approx}}$  and of the curve  $Y_{\text{mean}}$ .

The value of the error between  $y(t) = Y_{\text{mean}}$  and  $Y_{\text{approx}}$  given below is less than the value of  $C_1$  in (11) obtained with a fractional model,

$$C_2 = \frac{1}{N} \sum_{k=1}^N |y(k) - Y_{\text{approx}}(k)|^2 = 1.8714 \times 10^{-7}. \quad (19)$$

#### IV. ADDITION OF A PHENOMENON OF DESORPTION

The phenomenon of desorption is the release of particles from a surface. In order to capture this phenomenon, a desorption rate is added to the model (15). At each trial, every disk on the surface has a probability  $p$  of being desorbed. Taking into account this phenomenon combined with the RSA process gives the filling dynamic behavior of Fig. 13 with  $p = 10^{-4}$ . The filled surface in steady-state ( $\theta_{\infty} \approx 0.33$ ) is less important than in the case of Fig. 3 ( $\theta_{\infty} \approx 0.53$ ).

The model (15), thus, becomes

$$\dot{y}(t) = f(y)u(t) - \alpha[1 - y(t)], \quad (20)$$

where  $\alpha$  is the rate of desorption. For  $\alpha = 7.7 \times 10^{-5}$  and  $f$  given by (18), model (20) gives the result represented in Fig. 14. The value of the criterion is

$$C_3 = \frac{1}{N} \sum_{k=1}^N |y(k) - Y_{\text{des,fit}}(k)|^2 = 1.1158 \times 10^{-6}. \quad (21)$$

If the flow of particles is stopped during the process, the density of free area follows an exponential growth as it is illustrated in Fig. 15. The model (20) captures this behavior as is shown in Fig. 15.

The criterion value is

$$C_4 = \frac{1}{N} \sum_{k=1}^N |y(k) - Y_{\text{pulse,fit}}(k)|^2 = 1.7907 \times 10^{-5}. \quad (22)$$

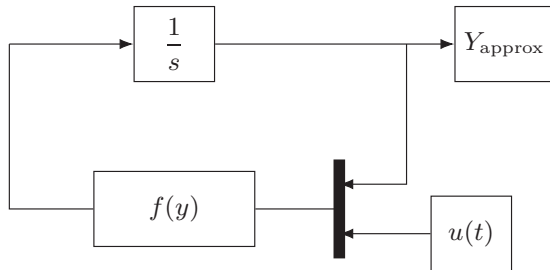
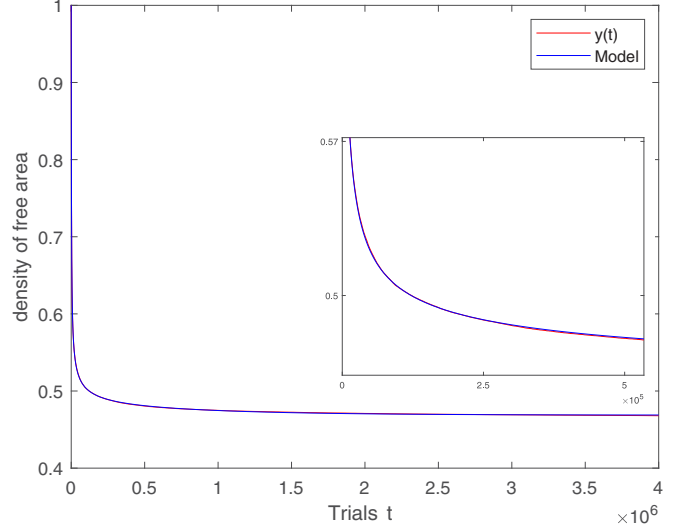


FIG. 11. Block diagram for simulation of model (15).

FIG. 12. Approximation for  $u(t) = 1$  (in blue) of the mean density  $Y_{\text{mean}}$  of free space (in red).

#### V. APPLICATION ON EXPERIMENTAL DATA

The experimental data used for this application are from adsorption of  $\text{CO}_2$  on copper hexacyanoferrate. These data come from the paper [39]. The copper hexacyanoferrate structure is composed of polydispersed particles with sizes ranging between 20 and 50 nm. The particles aggregate to form a porous network. The atmosphere is full of  $\text{N}_2$  at  $t = 0$ . The adsorption then occurs switching from  $\text{N}_2$  to  $\text{CO}_2$  atmosphere, without occupying specific sites ( $\text{CO}_2$  enters both large and small cavities). Switching back from  $\text{CO}_2$  to  $\text{N}_2$  starts the desorption phenomenon. The used instruments measure the weight of adsorbed  $\text{CO}_2$  over time. Figure 16 shows the kinetic of adsorption-desorption of  $\text{CO}_2$ .

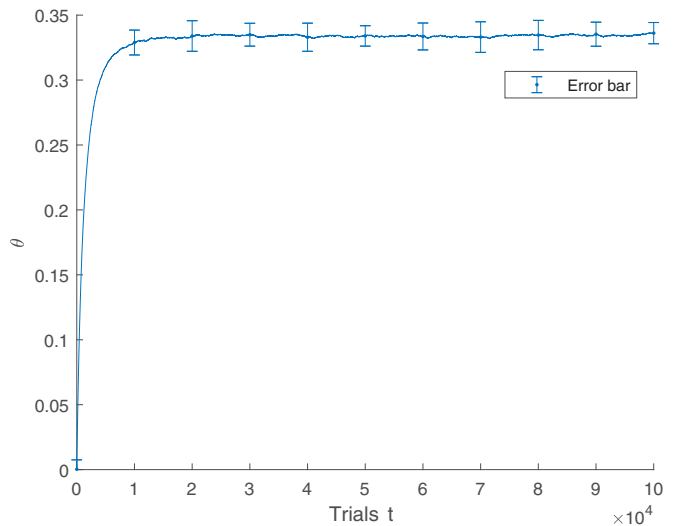


FIG. 13. Occupied density for adsorption-desorption.

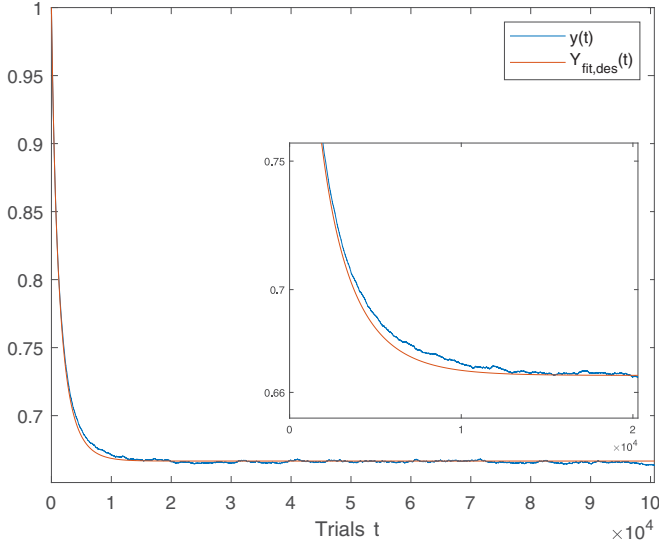


FIG. 14. Density of free area obtained by model (20) (in blue) compared to simulated data (in orange).

**A. Modeling of the adsorption part**

Using method described in Sec. III C, the adsorption part is modeled by the equation,

$$\dot{y}(t) = f(y)u(t), \tag{23}$$

with

$$f(y) = a_0 + a_1y + a_2y^2 + a_3y^3 + a_4y^4 + a_5y^5, \tag{24}$$

and here,  $t$  corresponds to the physical time. The parameters, obtained with FMINCON MATLAB'S function are given in Table II.

A comparison of the data and of the model response is performed in Fig. 17.

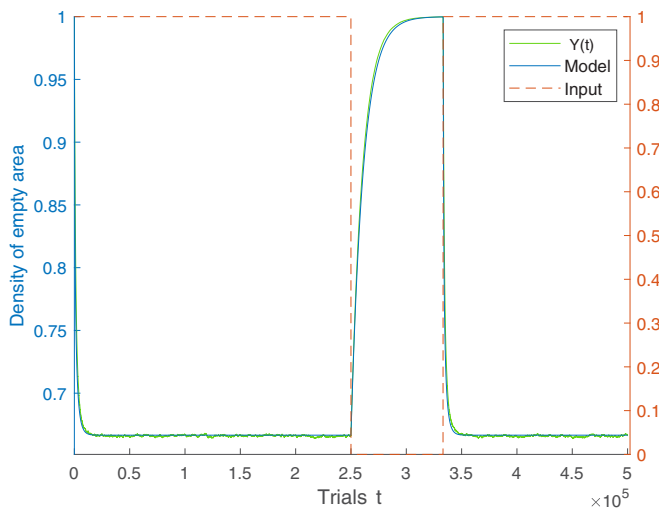


FIG. 15. Comparison between model (20) (in green) and simulated data (in blue) for a pulsed flow.

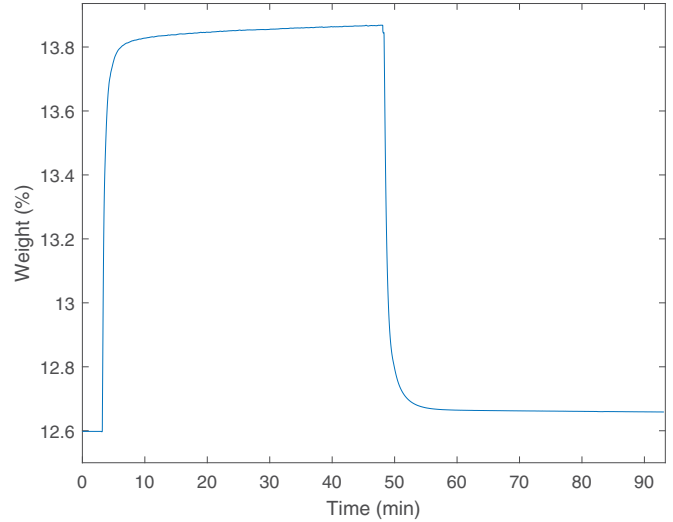


FIG. 16. CO<sub>2</sub> adsorption and desorption kinetic.

**B. Modeling of the pure desorption part**

With a simple first order desorption term of the form (20) and optimal value  $\alpha = 0.0129$ , the model does not fit the data as it is shown in Fig. 18. The quadratic error is  $C_5 = 2.3622 \times 10^{-4}$ .

To fit the desorption part as suggested in Ref. [39], it is proposed to use a second order model of impulse response,

$$A_{d1}e^{-k_1t} + A_{d2}e^{-k_2t}. \tag{25}$$

The parameters of this model are obtained through the minimization of a quadratic criterion that gives the following values:  $A_{d1} = 0.2342$ ,  $A_{d2} = 1.039$ ,  $k_1 = 0.0033$ , and  $k_2 = 0.0181$ .

A comparison of the second order model with the desorption data is shown in Fig. 19, after shifting time origin. For this second order, the quadratic error is  $C_6 = 2.8148 \times 10^{-5}$ .

**C. Modeling whole data**

The used desorption model suggests that a part of adsorbed particles desorb with a time constant  $k_1$  and the other part with a time constant  $k_2$ . To create a global model for adsorption and desorption, it is, thus, proposed to consider two bulks of adsorbed particles and to split model (23) in two parts,

$$\begin{aligned} \dot{x}_1 &= f_1(x_1)u(t) - k_1x_1, \\ \dot{x}_2 &= f_2(x_2)u(t) - k_2x_2, \\ y &= x_1 + x_2, \end{aligned} \tag{26}$$

with  $f_1$  and  $f_2$  as two polynomials to be reconstructed from the knowledge of function  $f$ .

In accordance with Eq. (25), let  $y_0 = y(t_0) = A_{d1} + A_{d2}$  be the initial value after the adsorption ends, where  $t_0$  denotes

TABLE II. Parameters of  $f$  from relation (24).

$a_0$	$a_1$	$a_2$	$a_3$	$a_4$	$a_5$
0.0247	0.0075	-0.0557	0.01954	0.0115	-0.0033

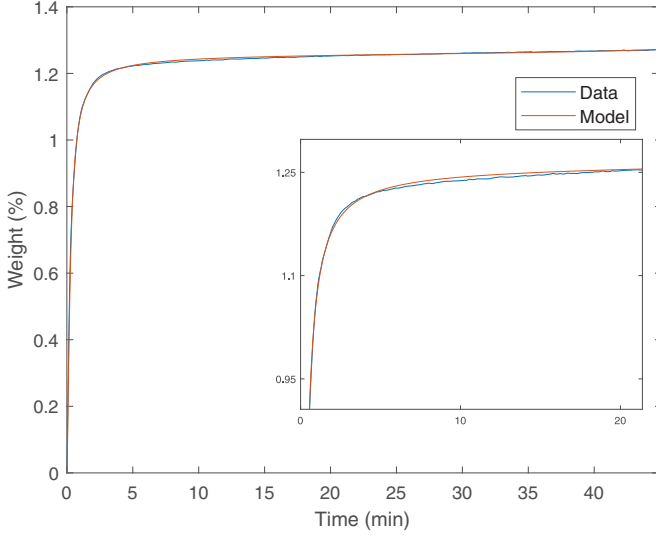


FIG. 17. Comparison of the adsorption part of the data and the model response.

this instant. The model must, thus, verify

$$x_1(t_0) = A_{d1}, \quad x_2(t_0) = A_{d2}. \quad (27)$$

This leads to choose

$$x_1(t_0) = A_{d1}, \quad x_2(t_0) = A_{d2}, \quad (28)$$

whose derivative is

$$\dot{x}_1(t) = \frac{A_{d1}}{y_0} \dot{y}(t), \quad \dot{x}_2(t) = \frac{A_{d2}}{y_0} \dot{y}(t). \quad (29)$$

Since  $\dot{y}(t) = f(y)$  [where  $f$  is the function given by relation (24) in which associated parameters are gathered in Table II], Eq. (30) can be rewritten

$$\begin{aligned} \dot{x}_1(t) &= \frac{A_{d1}}{y_0} f(y), \\ \dot{x}_2(t) &= \frac{A_{d2}}{y_0} f(y), \end{aligned} \Leftrightarrow \begin{cases} \dot{x}_1(t) = \frac{A_{d1}}{y_0} f\left(\frac{x_1(t)y_0}{A_{d1}}\right), \\ \dot{x}_2(t) = \frac{A_{d2}}{y_0} f\left(\frac{x_2(t)y_0}{A_{d2}}\right). \end{cases} \quad (30)$$

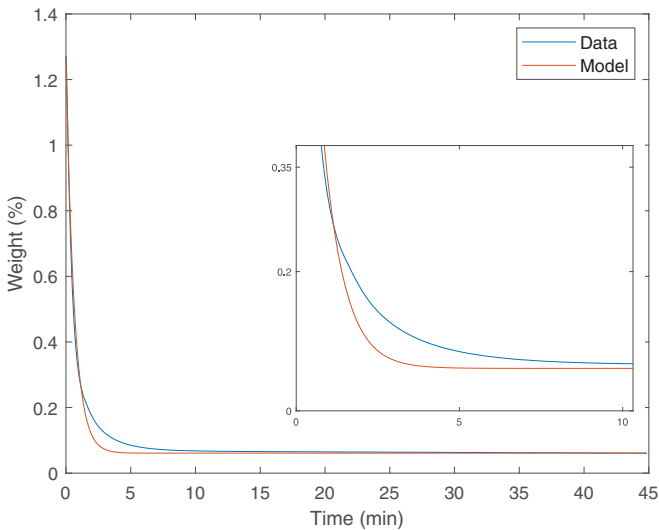


FIG. 18. Comparison of the desorption part of the data and the first order desorption model response.

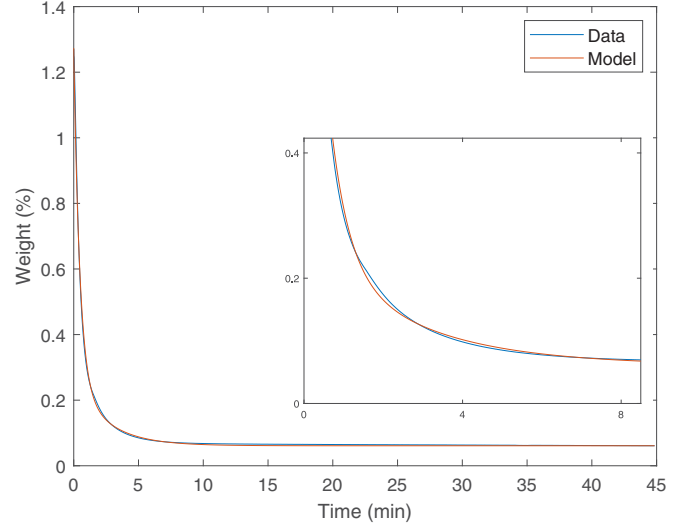


FIG. 19. Comparison of the desorption part of the data and the second order desorption model response.

Adding the desorption term and the flow  $u(t)$ , the previous system becomes

$$\begin{aligned} \dot{x}_1(t) &= \frac{A_{d1}}{y_0} f_1\left(\frac{x_1(t)y_0}{A_{d1}}\right) u(t) - k_1 x_1 \\ \dot{x}_2(t) &= \frac{A_{d2}}{y_0} f_2\left(\frac{x_2(t)y_0}{A_{d2}}\right) u(t) - k_2 x_2, \end{aligned} \quad (31)$$

in which  $f_1(X) = a'_0 + a'_1 X + a_2 X^2 + a_3 X^3 + a_4 X^4 + a_5 X^5$  and  $f_2(X) = a''_0 + a''_1 X + a_2 X^2 + a_3 X^3 + a_4 X^4 + a_5 X^5$  are two polynomials. The parameters  $a'_0$ ,  $a'_1$ ,  $a''_0$ , and  $a''_1$  are deduced from those of  $f$  as shown in the following, and the other parameters  $a_i$  are the same as in  $f$ . Adding the term of desorption affects the values of the parameters of degree 1. To avoid an impact on the adsorption part, the parameters  $a'_1$  in  $f_1$  and  $a''_1$  in  $f_2$  must verify

$$a'_1 = a_1 + k_1 \quad \text{and} \quad a''_1 = a_1 + k_2. \quad (32)$$

As the final value of the given data is not 0 (as depicted in Fig. 19) model (32) must be modified to take into account this constraint and becomes

$$\begin{aligned} \dot{x}_1(t) &= \frac{A_{d1}}{y_0} f_1\left(\frac{x_1(t)y_0}{A_{d1}}\right) u(t) - k_1(x_1 - y_f/2), \\ \dot{x}_2(t) &= \frac{A_{d2}}{y_0} f_2\left(\frac{x_2(t)y_0}{A_{d2}}\right) u(t) - k_2(x_2 - y_f/2), \end{aligned} \quad (33)$$

where  $y_f$  is the value of the weight at the end of desorption.

Adding  $y_f$  affects the parameters of degree 0 of model (32). To avoid an impact on the adsorption part, the following

TABLE III. Parameters of  $f_1$  and  $f_2$  of model (34).

$a'_0$	$a''_0$	$a'_1$	$a''_1$	$a_2$
0.0241	0.0239	0.0111	0.0279	-0.0557
$a_3$	$a_4$	$a_5$	$k_1$	$k_2$
0.0195	0.0115	-0.0033	0.0033	0.0181

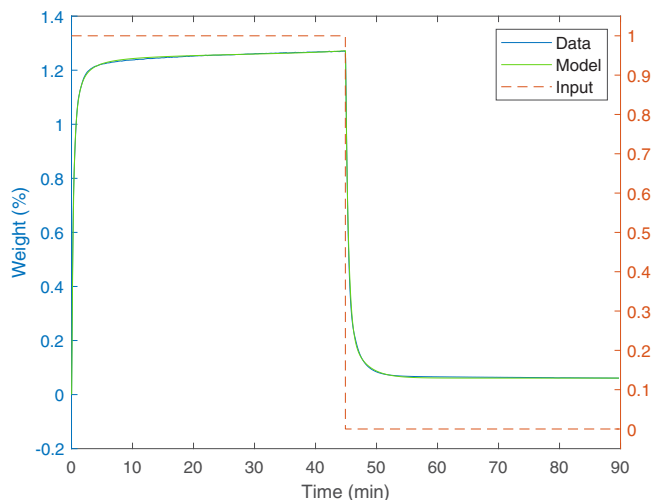


FIG. 20. Comparison of CO<sub>2</sub> adsorption and desorption data (in blue) with the model response (in red).

equality must hold:

$$a'_0 = a_0 - \frac{k_1 y_f}{2} \frac{y_0}{A_{d1}} \quad \text{and} \quad a''_0 = a_0 - \frac{k_2 y_f}{2} \frac{y_0}{A_{d2}}. \quad (34)$$

To summarize, the parameters obtained with this methodology for functions  $f_1$  and  $f_2$  are given in Table III.

A comparison of the data and of the response of model (34) is shown in Fig. 20. The quadratic error is  $C_7 = 2.1785 \times 10^{-5}$ .

In order to further improve the model, it is possible to increase again the order of the model that characterizes the pure desorption part and to use the exact same methodology.

## VI. CONCLUSION

Since many systems use the adsorption phenomenon especially for purification or measurement problems (gas sensors [6,7]), it is important to know how to model this phenomenon kinetic using dynamic models. This paper is a contribution to this modeling topic. In order to propose a relevant model, the RSA process, which describes a possible behavior of the particles during an adsorption phenomenon, is first investigated. This process shows kinetics in  $t^\nu$ ,  $\nu \in [0, 1]$  (power-law type kinetics). Moreover, the  $t^\nu$  kinetic is observed only in a middle time range of the RSA process. Such a behavior is not permitted with the models previously proposed in the literature. It is, thus, first proposed to capture the particular kinetic using a fractional model whose fractional behavior is only on a limited frequency band. However, introduction of a fractional model leads to several drawbacks: infinite dimensional model, initialization matters, inconsistencies with the studied phenomenon in terms of response to flux variations... Thus, in order to overcome these limitations, it is proposed to use a drift free control affine nonlinear model. The method to tune the parameters of this model is described, and the model efficiency is highlighted. Finally, the nonlinear model is enhanced to account for the desorption phenomenon and used to model data resulting from adsorption of CO<sub>2</sub> on copper hexacyanoferrate.

The authors intend to extend their results to the  $\nu$  dimension with  $\nu \in [2, 3]$  in order to take into account fractal surfaces.

## ACKNOWLEDGMENTS

We are thankful to D. O. Ojwang, J. Grins, and G. Svensson from the Department of Materials and Environmental Chemistry, Arrhenius Laboratory, Stockholm University to have provided us the adsorption and desorption data.

The authors declare that they have no conflict of interest.

- [1] S. Brunauer, L. S. Deming, W. E. Deming, and E. Teller, On a Theory of the van der Waals adsorption of gases, *J. Am. Chem. Soc.* **62**, 1723 (1940).
- [2] F. Rouquerol, J. Rouquerol, K. Sing, P. Llewellyn, and G. Maurin, *Adsorption by Powders and Porous Solids: Principles, Methodology and Applications*, 2nd ed. (Academic, Oxford, 2014).
- [3] A. Bonilla-Petriciolet, D. I. Mendoza-Castillo, and H. E. Reynel-Ávila, *Adsorption Processes for Water Treatment and Purification* (Springer, Berlin, 2017).
- [4] K. Czelej, K. Ćwieka, J. C. Colmenares, and K. Kurzydłowski, Insight on the interaction of methanol-selective oxidation intermediates with Au- or/and Pd-containing monometallic and bimetallic core@shell catalysts, *Langmuir* **32**, 7493 (2016).
- [5] K. Czelej, K. Ćwieka, and K. Kurzydłowski, CO<sub>2</sub> stability on the Ni low-index surfaces: Van der Waals corrected DFT analysis, *Catal. Commun.* **80**, 33 (2016).
- [6] H. Halil, P. Menini, and H. Aubert, Novel microwave gas sensor using dielectric resonator with SnO<sub>2</sub> sensitive layer, *Procedia Chem.* **1**, 935 (2009).
- [7] I. Nikolaou, H. Hallil, V. Conédéra, G. Deligeorgis, C. Dejous, and D. Rebiere, Inkjet-printed graphene oxide thin layers on love wave devices for humidity and vapor detection, *IEEE Sens. J.* **16**, 7620 (2016).
- [8] P. J. Flory, Intramolecular reaction between Neighboring Substituents of Vinyl Polymers, *J. Am. Chem. Soc.* **61**, 1518 (1939).
- [9] A. Rényi, On a one-dimensional problem concerning random space filling, *Pub. Math. Institut. Hungarian Acad. Sci.* **3**, 109 (1958).
- [10] P. Viot, G. Tarjus, S. Ricci, and J. Talbot, Random sequential adsorption of anisotropic particles. I. jamming limit and asymptotic behavior, *J. Chem. Phys.* **97**, 5212 (1992).
- [11] E. Hinrichsen, J. Feder, and T. Jøssang, Geometry of random sequential adsorption, *J. Stat. Phys.* **44**, 793 (1986).
- [12] J. Feder and I. Giaever, Adsorption of ferritin, *J. Colloid Interface Sci.* **78**, 144 (1980).
- [13] H. Bashiri and A. Shajari, Theoretical study of fractal-like kinetics of adsorption, *Adsorpt. Sci. Technol.* **32**, 623 (2014).
- [14] S. Lagergren, About the theory of so-called adsorption of soluble substances, *K. Sven. Vetenskapsakad. Handl.* **24**, 1 (1898).

- [15] R. Kopelman, Fractal reaction kinetics, *Science* **241**, 1620 (1988).
- [16] Y.-S. Ho and G. McKay, The kinetics of sorption of divalent metal ions onto sphagnum moss peat, *Water Res.* **34**, 735 (2000).
- [17] F. Brouers and O. Sotolongo-Costa, Generalized fractal kinetics in complex systems (application to biophysics and biotechnology), *Physica A* **368**, 165 (2006).
- [18] M. Haerifar and S. Azizian, Fractal-like adsorption kinetics at the solid/solution interface, *J. Phys. Chem. C* **116**, 13111 (2012).
- [19] R. H. Swendsen, Dynamics of random sequential adsorption, *Phys. Rev. A* **24**, 504 (1981).
- [20] V. Tartaglione, C. Farges, and J. Sabatier, Dynamical modelling of random sequential adsorption, in *Proceedings of European Control Conference (ECC'20), Saint Petersburg, 2020* (IEEE, Piscataway, NJ, 2020).
- [21] S. M. Ricci, J. Talbot, G. Tarjus, and P. Viot, Random sequential adsorption of anisotropic particles. II. low coverage kinetics, *J. Chem. Phys.* **97**, 5219 (1992).
- [22] Z. Adamczyk, J. Barbasz, and M. Cieřla, Kinetics of fibrinogen adsorption on hydrophilic substrates, *Langmuir* **26**, 11934 (2010).
- [23] M. Cieřla and J. Barbasz, Modeling of interacting dimer adsorption, *Surf. Sci.* **612**, 24 (2013).
- [24] P. M. Pasinetti, L. S. Ramirez, P. M. Centres, A. J. Ramirez-Pastor, and G. A. Cwilich, Random sequential adsorption on euclidean, fractal, and random lattices, *Phys. Rev. E* **100**, 052114 (2019).
- [25] P. Kubala, Random sequential adsorption of platonic and archimedean solids, *Phys. Rev. E* **100**, 042903 (2019).
- [26] R. C. Hart and F. D. A. Aaręo Reis, Random sequential adsorption of polydisperse mixtures on lattices, *Phys. Rev. E* **94**, 022802 (2016).
- [27] M. Cieřla and R. M. Ziff, Boundary conditions in random sequential adsorption, *J. Stat. Mech.* (2018) 043302.
- [28] G. Zhang and S. Torquato, Precise algorithm to generate random sequential addition of hard hyperspheres at saturation, *Phys. Rev. E* **88**, 053312 (2013).
- [29] J. Sabatier, O. Agrawal, and J. Tenreiro Machado, *Advances in Fractional Calculus: Theoretical developments and Applications in Physics and Engineering* (Springer, Berlin, 2007).
- [30] J. Sabatier, M. Merveillaut, R. Malti, and A. Oustaloup, On a representation of fractional order systems: Interests for the initial condition problem, in *3rd IFAC Workshop on Fractional Differentiation and its Applications, Ankara, Turkey 2008* (Elsevier, Amsterdam, 2008).
- [31] J. Sabatier, M. Merveillaut, R. Malti, and A. Oustaloup, How to impose physically coherent initial conditions to a fractional system? *Comm. Non. Sci. Num. Sim.* **15**, 1318 (2010).
- [32] M. Ortigueira and F. Coito, Initial Conditions: What Are We Talking About? in *3rd IFAC Workshop on Fractional Differentiation and its Applications, Ankara, Turkey, 2008* (Elsevier, Amsterdam, 2008).
- [33] J. Sabatier and C. Farges, Comments on the description and initialization of fractional partial differential equations using Riemann–liouville’s and Caputo’s definitions, *J. Comput. Appl. Math.* **339**, 30 (2018).
- [34] J. Sabatier, C. Farges, and J.-C. Trigeassou, Fractional systems state space description: Some wrong ideas and proposed solutions, *J. Vibr. Contr.* **20**, 1076 (2013).
- [35] J. Sabatier, Distributed time delay systems for power law type long memory behaviors modelling, *58th IEEE Conference on Decision and Control (CDC 2019), Nice, France, 2019* (IEEE, Piscataway, NJ, 2019), p. 7.
- [36] J. Sabatier, C. Farges, and V. Tartaglione, Some alternative solutions to fractional models for modelling long memory behaviours, *Mathematics* **8**, 196 (2020).
- [37] S. Sastry, *Nonlinear systems : Analysis, Stability, and Control*, Series on Interdisciplinary Applied Mathematics, Vol. 10 (Springer, Berlin, 1999).
- [38] A. Isidori, *Nonlinear Control Systems*, 3rd ed., Series on Communications and Control Engineering (Springer, Berlin, 1995).
- [39] D. O. Ojwang, J. Grins, and G. Svensson, The adsorption kinetics of CO<sub>2</sub> on copper hexacyanoferrate studied by thermogravimetric analysis, *Microporous Mesoporous Mater.* **272**, 70 (2018).